Published OnlineFirst April 24, 2012; DOI:10.1158/1078-0432.CCR-11-3213

Clinical Cancer Research

Coadministration of Epithelial Junction Opener JO-1 Improves the Efficacy and Safety of Chemotherapeutic Drugs

Ines Beyer, Hua Cao, Jonas Persson, et al.

Clin Cancer Res 2012;18:3340-3351. Published OnlineFirst April 24, 2012.

Published OnlineFirst April 24, 2012; DOI:10.1158/1078-0432.CCR-11-3213

Cancer Therapy: Preclinical

Clinical Cancer Research

Coadministration of Epithelial Junction Opener JO-1 Improves the Efficacy and Safety of Chemotherapeutic Drugs

Ines Beyer[1], Hua Cao[1], Jonas Persson[1], Hui Song[1], Maximilian Richter[1], Qinghua Feng[2], Roma Yumul[1], Ruan van Rensburg[1], Zongyi Li[1], Ronald Berenson[3], Darrick Carter[3], Steve Roffler[5], Charles Drescher[4], and André Lieber[1,2,3]

Abstract

Purpose: Epithelial junctions between tumor cells inhibit the penetration of anticancer drugs into tumors. We previously reported on recombinant adenovirus serotype 3–derived protein (JO-1), which triggers transient opening of intercellular junctions in epithelial tumors through binding to desmoglein 2 (DSG2), and enhances the antitumor effects of several therapeutic monoclonal antibodies. The goal of this study was to evaluate whether JO-1 cotherapy can also improve the efficacy of chemotherapeutic drugs.

Experimental Design: The effect of intravenous application of JO-1 in combination with several chemotherapy drugs, including paclitaxel/Taxol, nanoparticle albumin–bound paclitaxel/Abraxane, liposomal doxorubicin/Doxil, and irinotecan/Camptosar, was tested in xenograft models for breast, colon, ovarian, gastric and lung cancer. Because JO-1 does not bind to mouse cells, for safety studies with JO-1, we also used human DSG2 (hDSG2) transgenic mice with tumors that overexpressed hDSG2.

Results: JO-1 increased the efficacy of chemotherapeutic drugs, and in several models overcame drug resistance. JO-1 treatment also allowed for the reduction of drug doses required to achieve antitumor effects. Importantly, JO-1 coadmininstration protected normal tissues, including bone marrow and intestinal epithelium, against toxic effects that are normally associated with chemotherapeutic agents. Using the hDSG2-transgenic mouse model, we showed that JO-1 predominantly accumulates in tumors. Except for a mild, transient diarrhea, intravenous injection of JO-1 (2 mg/kg) had no critical side effects on other tissues or hematologic parameters in hDSG2-transgenic mice.

Conclusions: Our preliminary data suggest that JO-1 cotherapy has the potential to improve the therapeutic outcome of cancer chemotherapy. *Clin Cancer Res; 18(12); 3340–51. ©2012 AACR.*

Introduction

One of the key features of epithelial tumors is the presence of intercellular junctions, which link cells to one another, and act as barriers to the penetration of molecules with a molecular weight of 500 Da (1–3). Given that many chemotherapy drugs are larger than 500 Da, intercellular junctions represent a barrier to the penetration of these therapeutic agents into tumor. Several studies have shown that upregulation of epithelial junction proteins correlated with increased resistance to therapy, including therapy with monoclonal antibodies and chemotherapeutics (4, 5). One of these junction proteins is desmoglein 2 (DSG2). DSG2 is upregulated in malignant cells (6, 7). We found higher DSG2 immunoreactivity in breast cancer cells than in the surrounding normal epithelial tissue or tumor stroma cells (Supplementary Fig. S1).

Recently, we developed a recombinant protein (JO-1) that transiently triggers the opening of intercellular junctions in epithelial tumors. This work is based on our finding that DSG2 is a high-affinity receptor for a number of human adenoviruses (Ad), including Ad serotype 3 (8, 9). JO-1 is a self-dimerizing recombinant protein derived from the Ad3 fiber (10). JO-1 has a molecular weight of approximately 60 kDa and binds with picomolar avidity to DSG2. It can be readily produced in *Escherichia coli* and purified by affinity chromatography.

In mouse xenograft tumor models, we have shown that intravenous administration of JO-1 mediated cleavage of DSG2 dimers (between epithelial tumor cells) and activated intracellular signaling pathways, which reduced the expression of epithelial junction proteins in tumors (11). The

Authors' Affiliations: [1]University of Washington, Division of Medical Genetics; [2]University of Washington, Department of Pathology; [3]Compliment Corp.; [4]Fred Hutchinson Cancer Research Center, Seattle, Washington; and [5]Institute of Biomedical Sciences, Academia Sinica, Taipei, Taiwan

Note: Supplementary data for this article are available at Clinical Cancer Research Online (http://clincancerres.aacrjournals.org/).

Current address for I. Beyer: University of Duesseldorf, Department of OB/GYN, Germany

Corresponding Author: André Lieber, University of Washington, Division of Medical Genetics, Box 357720, Seattle, WA 98195. Phone: 206-221-3973; Fax: 206-685-8675; E-mail: lieber00@u.washington.edu

doi: 10.1158/1078-0432.CCR-11-3213

Published OnlineFirst April 24, 2012; DOI:10.1158/1078-0432.CCR-11-3213

Translational Relevance

Most cancers originate from epithelial tissues and retain features of differentiated epithelial cells such as tight junctions, that is, zipper-like structures that tightly link the individual malignant cells. This barricading feature can be used by tumors to exclude therapeutics from penetrating the tumor. We designed the recombinant protein JO-1 ("junction opener-1"). JO-1 binds to the junction protein desmoglein 2 (DSG2) in epithelial junctions, triggers the cleavage of adhesive DSG2 dimers, and activates intracellular signaling pathways resulting in a decreased expression of junction proteins. JO-1 coadministration increased the efficacy of several chemotherapy drugs in tumor models for breast, lung, and prostate cancer. Furthermore, JO-1 cotherapy allowed chemotherapy doses to be decreased without compromising the antitumor effects and provided protective effects to normal tissues. JO-1 cotherapy has the potential to improve both the efficacy of treatment and the life quality of cancer patients that receive chemotherapy.

morphologic changes triggered by JO-1 occurred within 1 hour after intravenous JO-1 injection and allowed for increased intratumoral penetration of the anti-Her2/*neu* monoclonal antibody trastuzumab (Herceptin) as well as for improved access to its target receptor, which is partly trapped in epithelial junctions (11). The effects of JO-1 on epithelial junctions translated into increased therapeutic efficacy of monoclonal antibodies (e.g., trastuzumab, cetuximab/Erbitux) against several xenograft tumor models, including breast, colon, ovarian, gastric, and lung carcinoma models (11).

Ad3 and its derivative JO-1 do not bind to mouse cells, implying that mouse DSG2 is not recognized (12). For safety studies with JO-1, we therefore used human DSG2 (hDSG2) transgenic mice that we recently generated. These mice express hDSG2 in a pattern and at a level similar to humans (12). For JO-1 efficacy studies, we also created a mouse epithelial breast cancer line that expressed hDSG2 and formed tumors in hDSG2-transgenic mice.

Using human xenograft and mouse tumor models, we showed that JO-1 increases the efficacy of a number of chemotherapy drugs that are widely used in the treatment of cancer patients.

Materials and Methods

JO-1

The production of JO-1 in *E. coli* and its purification have been described previously (10).

Cell lines

Breast cancer BT474-M1 cells and MDA-MB-231 [American Type Culture Collection (ATCC), HTB-26] were cultured in Dulbecco's Modified Eagle's Medium/F12 with 10% FBS, 1% penicillin/streptomycin and 2 mmol/L L-glutamine. Breast cancer HCC1954 (ATTC; CRL-2338), lung cancer A549 (ATCC; CCL-185), prostate cancer 22Rv1 (ATCC; CRL-2505), and mouse mammary carcinoma (MMC) and MMC-hDSG2 cells (12) were cultured in RPMI with 10% FBS and 1% penicillin/streptomycin. To achieve cell polarization, 1.4×10^5 T84 cells (ATCC; CCL-248) were cultured in collagen-coated 6.5 mm Transwell inserts (0.4 μm pore size; Costar Transwell Clears) for a period of 14 to 20 days until transepithelial resistance was stable (8).

Tissues

The preparation of optimum cutting temperature and paraffin sections has been described previously (12). Bones were decalcified before embedding in paraffin. A list of antibodies used for immunohistochemistry and flow cytometry is available in the Supplementary Information. Images were taken with a Leica DMLB microscope (Wetzlar), using Leica DFC300 FX Digital camera and Leica Application Suite Version 2.4.1 R1 software.

Animal studies

All experiments involving animals were conducted in accordance with the institutional guidelines set forth by the University of Washington. Breast cancer xenografts were established by injecting tumor cells into the mammary fat pad of CB17 SCID-beige mice. Prostate and lung cancer models were created by subcutaneous injection. hDSG2-transgenic mice were generated by knock-in of approximately 90 kb of human DNA containing the DSG2 gene together with its regulatory regions. The mice contain 2 copies of the hDSG2 gene and express hDSG2 in a pattern similar to humans (12). MMC-hDSG2 tumors were generated by subcutaneous injection of MMC-hDSG2 cells mixed with Matrigel. JO-1 was intravenously injected 1 hour before the application of chemotherapy drugs. Tumor volumes were measured 3 times a week. Each treatment group consisted of a minimum of 5 mice. Animals were sacrificed, and the experiment terminated when tumors in one of the groups reached a volume of 800 mm^3 or tumors displayed ulceration. To produce anti–JO-1 antibodies, hDSG2-transgenic mice received 3 subcutaneous injections of 5 μg JO-1 at days 0, 3, and 14. Serum was collected 4 weeks later and analyzed for JO-1–specific antibodies by Western blot.

ELISA

To measure liposomal doxorubicin/Doxil concentrations, mice were sacrificed and blood was flushed from the circulation with 10 mL PBS. Tissues were homogenized in PBS/0.1% Tween 20/protease inhibitors. Anti-PEG (PEG, polyethylene glycol) antibody AGP4 (13) was used as a capture antibody. Binding was detected with anti-PEG antibody 3.3.-biotin (13) followed by a streptavidin–HRP (HRP, horseradish peroxidase) conjugate. To measure JO-1 in tissue lysates, an anti-Ad3 fiber knob antibody (8) was used as capture antibody. JO-1 binding was detected using a mouse monoclonal antibody against the 6xHis tag of JO-1, followed by anti-mouse IgG-HRP (IgG, immunoglobulin G).

Published OnlineFirst April 24, 2012; DOI:10.1158/1078-0432.CCR-11-3213

Statistical analysis

All results are expressed as mean ± SD. Two-way ANOVA for multiple testing was applied. Animal numbers and *P* values are indicated in the figure legends.

Results

The goals of this study were to show that: (i) JO-1 cotherapy specifically increases the antitumor efficacy of chemotherapeutic drugs in epithelial tumors and (ii) JO-1 cotherapy allows dose sparing of chemotherapeutics, which in turn reduces adverse side effects associated with chemotherapy. Our study included the following chemotherapy drugs: (i) paclitaxel/Taxol (molecular weight 856.9 Da). Paclitaxel is used to treat patients with lung, ovarian, breast, head, and neck cancer and advanced forms of Kaposi sarcoma. (ii) Nanoparticle albumin–bound paclitaxel nab-paclitaxel/Abraxane (effective size of the particle: ~130 nm). nab-Paclitaxel has recently been approved for the treatment of recurrent breast cancer. (iii) Irinotecan/Camptosar (molecular weight 586.7 Da). Irinotecan is used to treat colon and lung cancer. The most significant adverse effects of irinotecan are severe diarrhea and immunosuppression. (iv) Liposomal doxorubicin/Doxil (effective size of the particle: ~90 nm) is a PEG coated, liposome-encapsulated form of doxorubicin. Liposomal doxorubicin is used in the treatment of several epithelial tumors, including ovarian and breast cancers. To test the effect of JO-1 on chemotherapy, we studied 5 xenograft models using immunodeficient CB17-SCID-beige mice carrying tumors derived from human tumor cell lines. The epithelial phenotype and existence of tight junctions in the xenograft tumors was confirmed by immunohistochemical detection of the junction proteins DSG2, E-cadherin, ZO-1, and claudin 7 (8, 14; data not shown). Furthermore, we used an hDSG2-transgenic mouse model with orthotopic breast tumors expressing hDSG2. The doses of chemotherapy drugs used in our studies were based on information reported in previous publications (15). These doses reflected doses used in patients converted through allometric scaling to the weight of mice. Mice with preestablished tumors were intravenously injected with either JO-1 (2 mg/kg) or PBS 1 hour before intravenous/intraperitoneal administration of the chemotherapeutic agents. This regime had been found to be optimal in the combination therapy of JO-1 with monoclonal antibodies (14).

JO-1 improves the efficacy of chemotherapeutic drugs and can overcome drug resistance

Cotherapy of JO-1 and paclitaxel was first tested in the BT474-M1 breast cancer model (Fig. 1A). These tumors are resistant to paclitaxel. JO-1 cotherapy was able to halt tumor growth and thus overcame resistance to paclitaxel treatment. JO-1/paclitaxel cotherapy was then evaluated in the MDA-MB-231 breast cancer model (Supplementary Fig. S2). JO-1 injection alone had no significant therapeutic effect. Antitumor effect of paclitaxel alone was found, which was significantly enhanced by preinjection of JO-1. The MDA-MB-231 tumor model was also used to study the effect of JO-1 on nab-paclitaxel therapy (Fig. 1B). Nab-paclitaxel was not significantly more effective than paclitaxel in decreasing tumor growth in this tumor model. Similar to paclitaxel, combining JO-1 with nab-paclitaxel therapy increased its therapeutic effects, whereby the enhancing effect was significantly more pronounced for nab-paclitaxel. This suggests that the enhancement in therapeutic efficacy through JO-1 is stronger for larger, particle-based drugs. Similarly, JO-1 was shown to enhance the antitumor effects of liposomal doxorubicin in the prostate cancer model (Fig. 1C) and the model with subcutaneous tumors derived from primary ovarian cancer cells (ref. 16; Supplementary Fig. S3A). The residual tumor mass seen in JO-1 plus chemotherapy treated mice in Fig. 1A and C only contained tumor stroma and infiltrating leukocytes upon histologic inspection. Furthermore, in these studies, no tumor growth relapse was observed when mice were followed for a total of 60 days after the start of the experiment.

Paclitaxel, nab-paclitaxel, and liposomal doxorubicin all have molecular weights of more than 500 Da; therefore, intercellular junctions could represent physical barriers to the penetration of these drugs into tumors. If our hypothesis is correct, JO-1–mediated junction opening should have less effects on drugs smaller than 500 Da. To test this hypothesis, we evaluated the effects of JO-1 cotherapy on cisplatin, which has a molecular weight of 300 Da in models of breast (Fig. 1D), lung (Fig. 1E), and ovarian (Supplementary Fig. S3B). Notably, it has been shown before that the cell lines used in this study were sensitive to cisplatin in culture (16, 17). Further support for the hypothesis that larger drugs benefit more from JO-1 cotherapy comes from a study with cyclophosphamide (molecular weight 260), in which JO-1 also did not significantly enhance the therapeutic effect (Fig. 1F).

JO-1 allows for lowering chemotherapy doses and provides protective effects to normal tissues

Our second hypothesis is that JO-1 cotherapy would allow decreasing the doses of chemotherapeutics required to achieve therapeutic efficacy. To test this, we injected chemotherapeutic agents at different dose levels into tumor-bearing mice and monitored tumor volumes as well as toxicity parameters, including blood cell counts, blood chemistry, and tissue histology. First, we tested JO-1 in combination with the topoisomerase inhibitor irinotecan in the A549 lung cancer model described above (Fig. 2A–D). As observed for the other drugs, JO-1 significantly increased the therapeutic efficacy of irinotecan. A combination of a low dose of irinotecan (37.5 mg/kg) and JO-1 was significantly more effective than "standard" dose (75 mg/kg) irinotecan alone, indicating that JO-1 allows for lowering the effective drug dose (Fig. 2A). Irinotecan treatment caused thrombocytopenia and leukopenia as a result of myelotoxicity, although there was no significant difference in the severity of leukopenia or thrombocytopenia observed in animals treated at the 2 different doses (Fig. 2B). Coadministration of JO-1 had a myeloprotective effect. It

Published OnlineFirst April 24, 2012; DOI:10.1158/1078-0432.CCR-11-3213

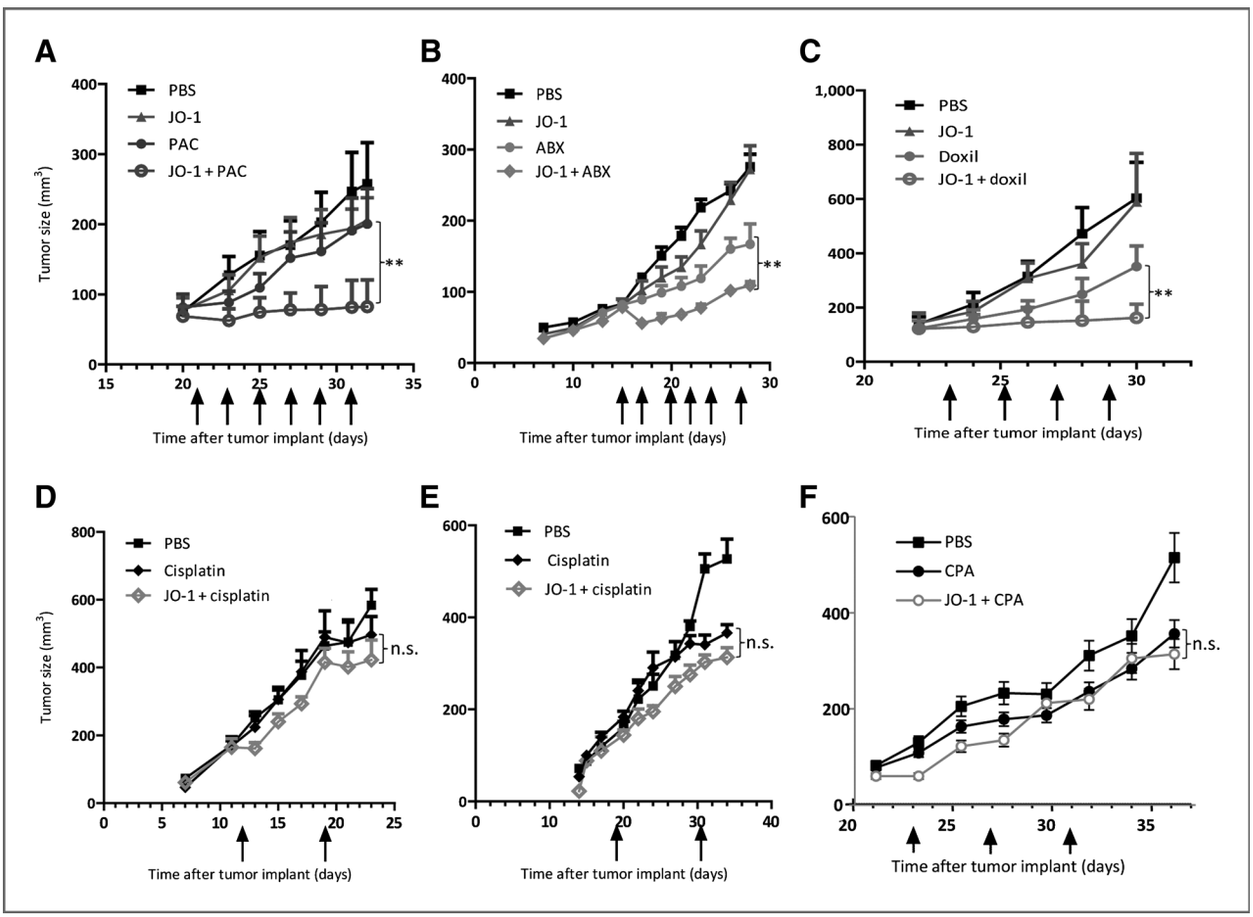

Figure 1. JO-1 improves efficacy of chemotherapy agents in several cancer models. A, a total of 4×10^6 BT474-M1 cells were injected into the mammary fat pad of CB17-SCID/beige mice. Twenty-one days later when tumors reached a volume of approximately 80 mm^3, mice received an intravenous injection of 50 μg of JO-1 (2 mg/kg) or PBS, followed by an intravenous injection of paclitaxel (PAC; 5 mg/kg) or PBS 1 hour later. The treatment was given every other day until day 31. Animals received a total of 6 doses of cotherapy (marked by arrows). $n = 5$. **, $P < 0.05$. B, MDA-MB-231 tumors were established as described in (A). nab-Paclitaxel (Abraxane-ABX) at a dose of 5 mg/kg was injected intravenously 1 hour after JO-1 injection. The treatment was repeated on days 17, 20, 22, 24, and 27. $n = 5$. ABX versus JO-1 + ABX: **, $P < 0.01$ for all time points after day 22. C, a similar study was carried out with a prostate cancer cell line. A total of 2×10^6 22Rvl cells were injected subcutaneously into the flank of CB17-SCID/beige mice. When tumors reached a volume of approximately 130 mm^3, mice received an intravenous injection of 50 μg JO-1 (2 mg/kg) or PBS, followed by an intravenous injection of liposomal doxorubicin (Doxil; 3 mg/kg) or PBS 1 hour later (day 21). The treatment was repeated every other day until day 29. $n = 5$. Doxil versus JO-1 + Doxil: **, $P < 0.01$ for day 30. D, in a Her2/neu-positive breast cancer model, we tested whether JO-1 increased the therapeutic effects of cisplatin. In this experiment, 4×10^6 HCC1954 cells were injected into the mammary fat pad. The treatment was started on day 12, when tumors had reached a volume of 160 mm^3. Mice were injected with JO-1 (2 mg/kg) or PBS intravenously and followed by intravenous injection of cisplatin (2 mg/kg; this dose of cisplatin is routinely used in preclinical studies (25) or PBS 1 hour later. The injections was repeated on day 19. $n = 5$. The differences of tumor growth between animal treatment groups were not significant. E, mice were injected subcutaneously with 4×10^6 lung cancer A549 cells. The treatment was started on day 12, when tumors had reached a volume of approximately150 mm^3. Mice were injected with JO-1 (2 mg/kg) or PBS intravenously and followed by intravenous injection of cisplatin (2 mg/kg) or PBS 1 hour later. The injections was repeated on day 30. $n = 5$. The differences of tumor growth between "cisplatin" and "JO-1 + cisplatin" were not significant. F, mice carrying tumors derived from breast cancer cells MDA-MB-231 cells (see A) were intraperitoneally injected once a week with cyclophosphamide (CPA; 100 mg/kg) and with and without JO-1. Note that MDA-MB-231 cells are sensitive to CPA *in vitro* (17). $n = 5$. The difference between "CPA" and "JO-1 + CPA" was not significant.

prevented the decrease in platelet and white blood cell counts, which was especially noteworthy at the higher drug dose. Compared with control animals, spleens were significantly smaller in irinotecan-treated animals but not in animals that received irinotecan in combination with JO-1. Splenic atrophy in irinotecan-treated animals is also visible in microscopic analysis of spleen sections (Fig. 2C). JO-1 also reduced irinotecan-mediated damage to the intestinal epithelium (Fig. 2D).

Next, we evaluated nab-paclitaxel in the MDA-MB-231 breast cancer model. nab-Paclitaxel was administered at 2 different dose levels (5 and 10 mg/kg) alone or in combination with JO-1 (Fig. 2E–F). JO-1 cotherapy significantly increased the antitumor effects of nab-paclitaxel (Fig. 2E). The combination of JO-1 plus nab-paclitaxel (5 mg/kg) was significantly more effective than nab-paclitaxel alone given at a dose of 10 mg/kg. JO-1 plus nab-paclitaxel (10 mg/kg) halted tumor growth. Compared with

Published OnlineFirst April 24, 2012; DOI:10.1158/1078-0432.CCR-11-3213

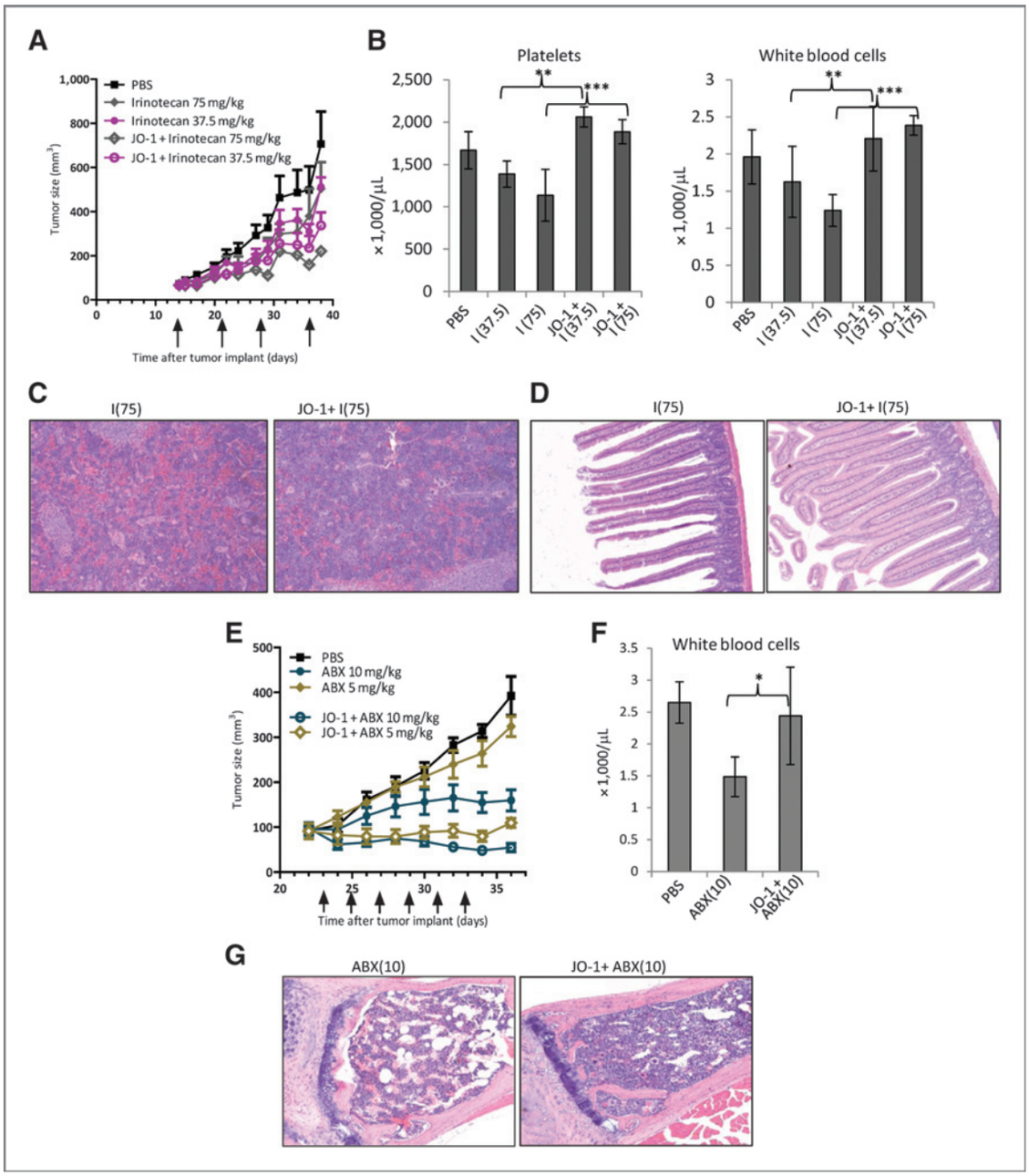

Figure 2. JO-1 allows for lowering of chemotherapeutic doses and mitigates toxic side effects. A–D, irinotecan: immunodeficient CB17-SCID/beige mice were injected subcutaneously with 4×10^6 A549 cells. JO-1 (2 mg/kg) was injected at day 14 intravenously (when tumors had a volume of 65 mm^3) followed by an intraperitoneal injection of irinotecan (I) at 2 different dose levels (75 or 37.5 mg/kg) or PBS 1 hour later. The treatment was repeated weekly until day 36. A, tumor volumes. $n = 5$. Irinotecan (37.5 mg/kg) versus JO-1 + irinotexan (37.5 mg/kg): $P < 0.01$ on day 38; $P < 0.001$ day 38 for 75 mg/kg. B–D, at the end of the monitoring period, animals were sacrificed and blood cell counts as well as tissue histology were analyzed. I(37.5)—irinotecan (37.5 mg/kg), I(75)—irinotecan (75 mg/kg). B, platelet and white blood cell counts in treated mice at the day of sacrifice (day 38). $n = 5$, irinotecan (37.5 mg/kg) versus JO-1 + irinotexan (37.5 mg/kg): **, $P < 0.01$. Irinotecan (75 mg/kg) versus JO-1 + irinotexan (75 mg/kg): ***, $P < 0.001$. C, representative spleen sections, hematoxylin and eosin (H&E) stained. Note depletion of cells in germinal centers in I(75)-treated mice. Magnification × 20. D, representative intestine sections. E–G, nab-paclitaxel (ABX): immunodeficient CB17-SCID/beige mice were subcutaneously injected with 3×10^6 MDA-MB-231 cells. Mice were treated from day 23 on, when the tumors reached a volume of approximately 90 mm^3. They were injected every other day with JO-1 (2 mg/kg) or PBS intravenously, followed 1 hour later by nab-paclitaxel (ABX) at different dose levels (10 and 5 mg/kg). E, tumor volumes. $n = 5$. ABX (5 mg/kg) versus JO-1 + ABX (5 mg/kg): $P < 0.001$ from day 28 on; ABX (10 mg/kg) versus JO-1 + ABX (10 mg/kg): $P < 0.01$ from day 30 on. F, white blood cell counts in treated mice at the day of sacrifice (day 36). $n = 5$, ABX(10) versus JO-1 + ABX(10): *, $P < 0.05$. G, representative sternum sections. H&E stained. Note depletion of bone marrow cells in ABX(10)-treated mice. H–K, liposomal doxorubicin (Doxil). A total of 4×10^6 A549 cells were injected subcutaneously into CB17-SCID/beige mice. Once the tumor reached a volume of 65 mm^3, the mice were injected intravenously with 2 mg/kg JO-1 or PBS, followed by an intravenous injection of liposomal doxorubicin (1 or 3 mg/kg) or PBS 1 hour later. The treatment was repeated on day 17, 20, and 22.

Published OnlineFirst April 24, 2012; DOI:10.1158/1078-0432.CCR-11-3213

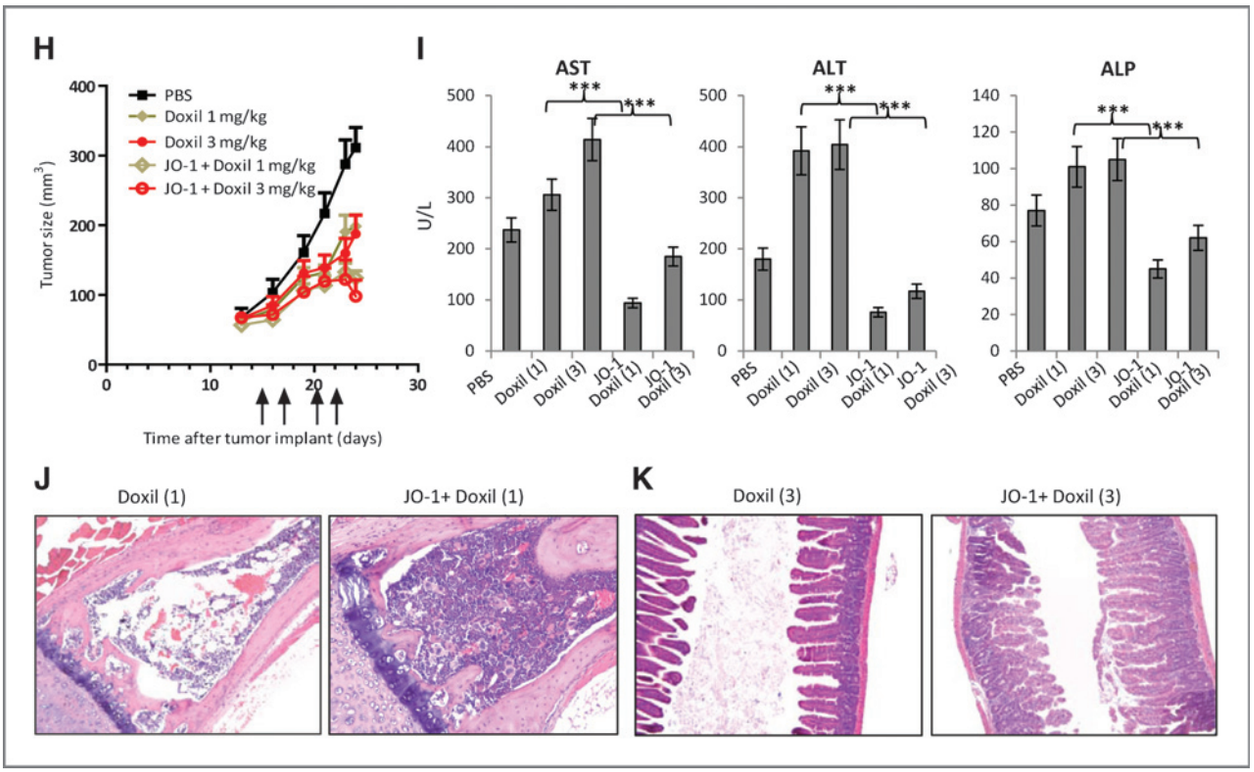

Figure 2. (*Continued*) H, tumor volumes. $n = 5$. Liposomal doxorubicin (1 mg/kg) intravenously versus JO-1 + liposomal doxorubicin (1 mg/kg): $P < 0.05$ from day 23 on; liposomal doxorubicin (3 mg/kg) versus JO-1 + liposomal doxorubicin (3 mg/kg): $P < 0.05$ from day 24 on. I–K, toxicology studies Doxil (1)—liposomal doxorubicin (1 mg/kg), Doxil (3)—liposomal doxorubicin (3 mg/kg). I, serum enzymes: AST, ALT, and alkaline phosphatase (ALP). $n = 3$. Liposomal doxorubicin (1 mg/kg) versus JO-1 + liposomal doxorubicin (1 mg/kg): **, $P < 0.01$; liposomal doxorubicin (3 mg/kg) versus JO-1 + liposomal doxorubicin (3 mg/kg): **, $P < 0.01$. The elevated transaminase levels in PBS-treated control animals could be explained by the presence of relatively large xenograft tumors in these mice which potentially can produce factors that act on hepatocytes. J, representative sternum sections. K, representative intestine sections.

paciltaxel, nab-paclitaxel showed a better safety profile based on blood cell analysis (data not shown). However, the highest dose of nab-paclitaxel (10 mg/kg) still decreased the white blood cell count, which was prevented by JO-1 pretreatment (Fig. 2F). The myeloprotective effect was also shown in sternum sections. In contrast to the depletion of bone marrow cells seen in mice treated with ABX alone, animals that received JO-1/ABX cotherapy displayed a normal histology (Fig. 2G). Notably, no toxic side effects of nab-paclitaxel were found in the other tissues analyzed, that is, intestine, kidney, and spleen.

The third model involved liposomal doxorubicin in the A549 lung cancer model (Fig. 2H–K). Similar to the results above, JO-1 pretreatment significantly improved liposomal doxorubicin therapy at both dose levels of the chemotherapy drug (1 and 3 mg/kg; Fig. 2H). JO-1 mitigated adverse side effects induced by liposomal doxorubicin. For example, markers for liver damage, including aspartate aminotransferase (AST), alanine aminotransferase (ALT), and alkaline phosphatase (ALP) were significantly decreased in animals treated with JO-1 and liposomal doxorubicin than in mice treated with liposomal doxorubicin alone (Fig. 2I). Severe tissue damage, caused by liposomal doxorubicin, found in the bone marrow and intestinal epithelium was greatly reduced in mice that received JO-1 injections (Fig. 2J and K).

Importantly, in all 3 studies shown in Fig. 2, we found that JO-1 cotherapy greatly reduced the toxic side effects associated with chemotherapy. We speculate that the ability of JO-1 to open up intercellular junctions in tumors and increase the uptake of chemotherapeutics reduces the drug exposure to normal tissue thus providing a larger therapeutic window. In support of this speculation, using an ELISA to measure PEGylated compounds in tissues (13), we found significantly more liposomal doxorubicin in tumors and less in other tissues in mice that received JO-1 prior to intravenous liposomal doxorubicin injection (Fig. 3A). Immunofluorescence analysis of tissue sections revealed more Doxil signals in tumors of JO-1 + Doxil-treated mice (Fig. 3B). In these animals, Doxil was found more dispersed over a greater distance from blood vessels, suggesting better intratumoral penetration and absorption by tumor tissue (Fig. 3B).

JO-1 biodistribution, tumor therapy, and safety studies in hDSG2-transgenic mice

A more adequate model for safety and efficacy studies with JO-1 are hDSG2-transgenic mice with MMC-hDSG2

Published OnlineFirst April 24, 2012; DOI:10.1158/1078-0432.CCR-11-3213

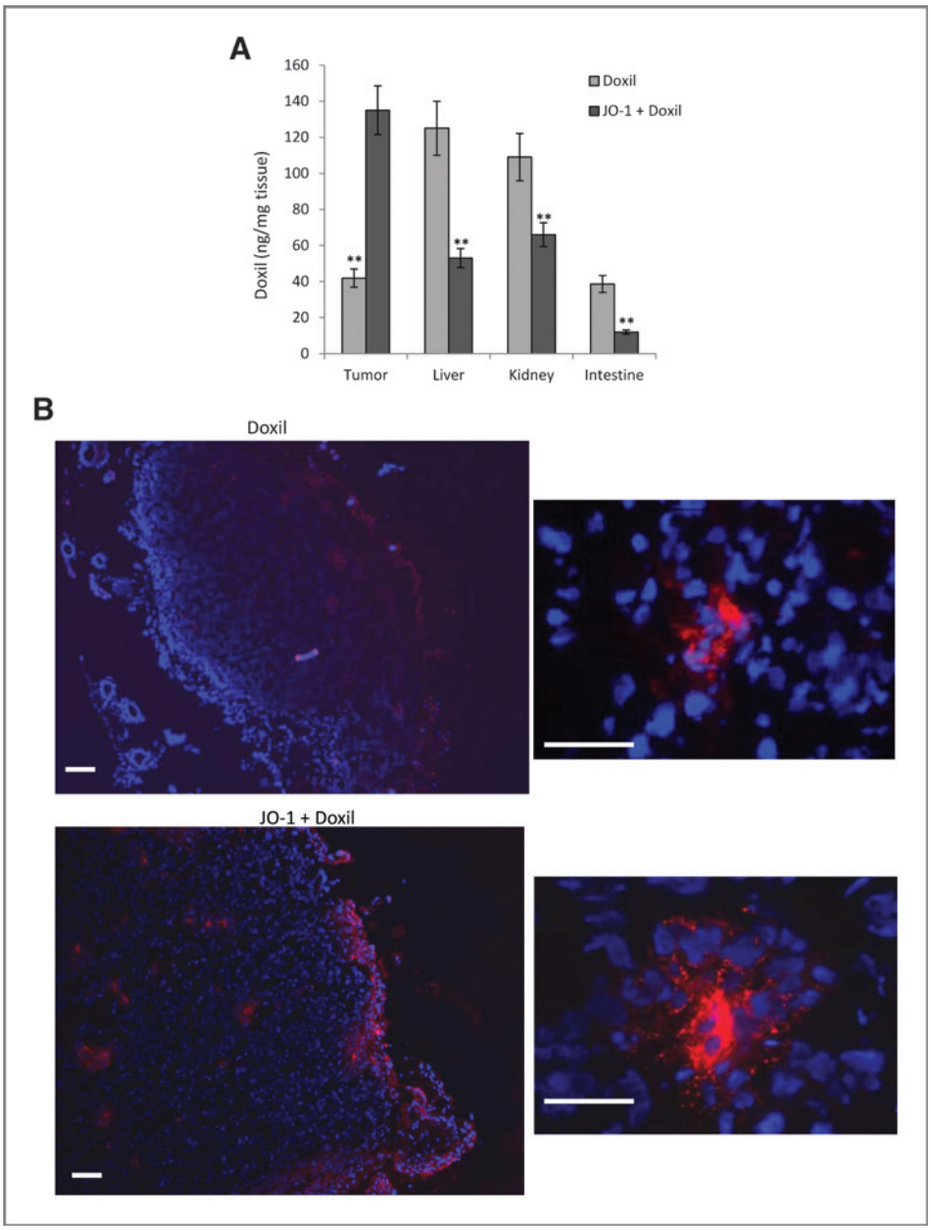

Figure 3. Liposomal doxorubicin/Doxil biodistribution. Mice carrying HCC1954 tumors were intravenously injected with PBS, Doxil (1 mg/kg), or JO-1 (2 mg/kg) followed by Doxil 1 hour later. Two hours after PBS or Doxil injection, mice were sacrificed, blood was flushed from the system, and organs were collected to analyze the presence of Doxil in tissues using antibodies against PEG. A, tissue lysates were subjected to ELISA for JO-1. $n = 3$. The differences between the 2 groups are significant (**, $P < 0.01$). B, immunfluorescence analysis of tumor sections with anti-PEG antibodies. Scale bar, 20 μm. Notably, free PEG is poorly detected by ELISA or immunohistochemistry (13). Effective binding is greatly enhanced in PEG conjugates such as Doxil.

tumors. JO-1 binds to MMC-DSG2 cells and triggers reorganization of junctions in a similar way as seen in human epithelial cells, indicating that JO-1 signaling through hDSG2 can override junction regulation in mouse cells (12). Transplantation of MMC-hDSG2 cells into the mammary fat pad of hDSG2-transgenic mice resulted in tumors that resembled key features of breast cancer in humans, for example, nests of hDSG2^{bright} epithelial cells that were surrounded by tumor stroma (Fig. 4A). Intravenous injection of JO-1 resulted in efficient accumulation of JO-1 in MMC-hDSG2 tumor nests as seen on tumor sections analyzed 6 hours after injection (Fig. 4A). Immunoreactive JO-1 was also found in epithelial cells of the intestine in hDSG2-transgenic mice (Fig. 4B), which is consistent with our recent biodistribution study with Ad3-GFP virus (12). We measured JO-1 concentrations in tissue and tumor lysates by ELISA at 6 hours after injection in the following 4 groups of animals: (i) hDSG2-transgenic mice with MMC-hDSG2 tumors (Fig. 4C; "hDSG2-pos"), (ii) hDSG2-transgenic mice without tumors (Fig. 4D; "hDSG2-pos"), (iii) nontransgenic littermates with MMC tumors (Fig. 4C; "hDSG2-neg"), and (iv) nontransgenic littermates without tumors (Fig. 4D; "hDSG2-neg"). We found highly selective, hDSG2-dependent accumulation of JO-1 in MMC-hDSG2 tumors established in hDSG2-transgenic mice. About 10-fold less JO-1 was found in the intestine and colon of hDSG2-transgenic mice. JO-1 was also detected in the liver and spleen of both hDSG2-positive and hDSG2-negative

Published OnlineFirst April 24, 2012; DOI:10.1158/1078-0432.CCR-11-3213

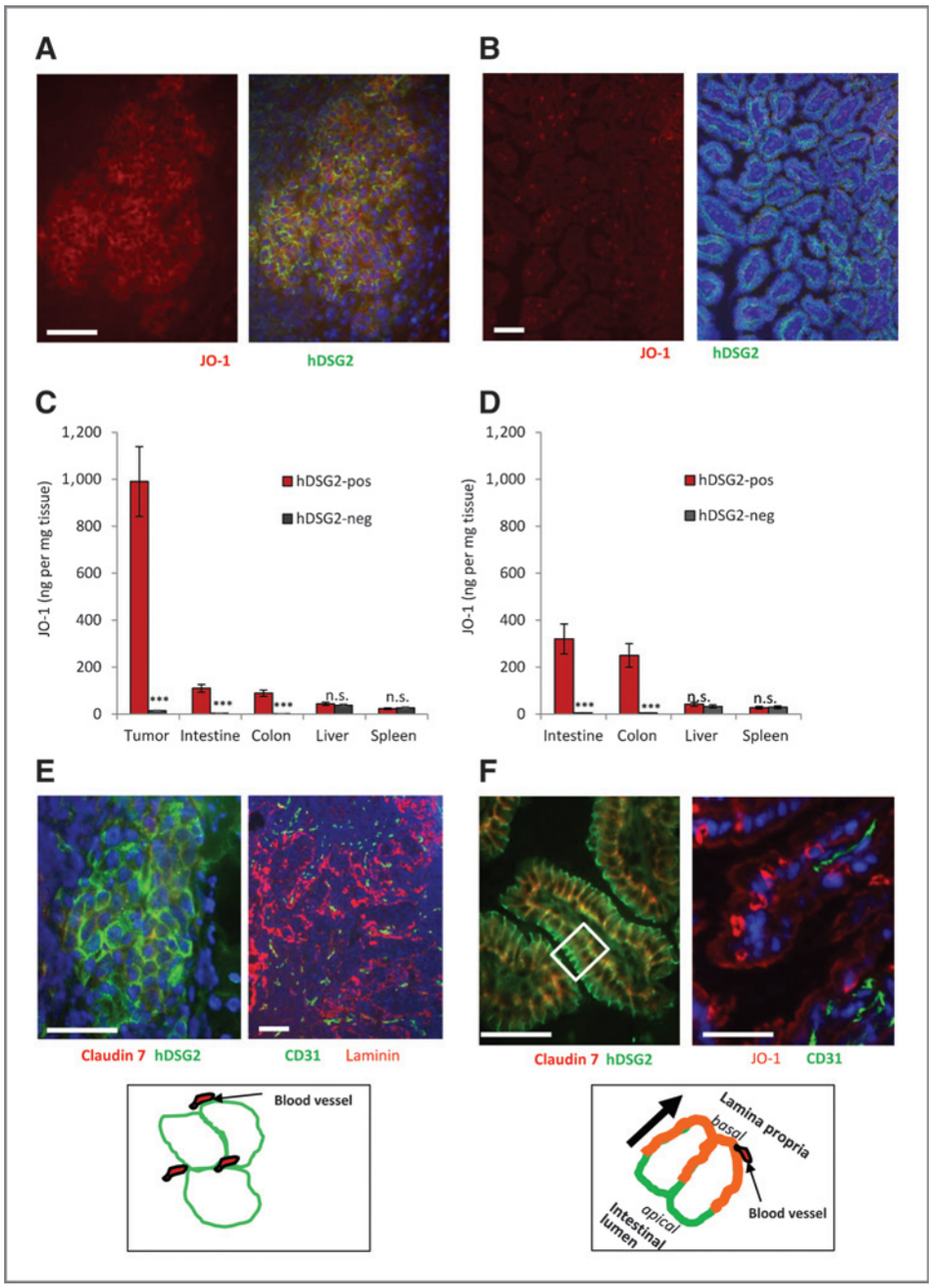

Figure 4. JO-1 biodistribution studies in hDSG2-transgenic mice. A–C, a total of 4×10^6 MMC-hDSG2 cells were injected into the mammary fat pad of hDSG2-transgenic mice. When tumors reached a volume of 100 mm^3, JO-1 (2 mg/kg) was injected intravenously. Mice were sacrificed 6 hours later, blood was removed from the circulation, and organs were harvested. A and B, sections of MMC-hDSG2 tumors and intestine stained for JO-1 (red) and hDSG2 (green). C and D). JO-1 biodistribution: JO-1 (2 mg/kg) was injected intravenously. Six hours later, blood was flushed from the circulation and tissue lysates were analyzed for JO-1 by ELISA. $n = 3$. ***, $P < 0.001$; n.s., nonsignficant. E and F, tumor (E) and intestine (F) sections from MMC-hDSG2 tumor bearing hDSG2-transgenic mice were stained for the adherens junction marker claudin 7 (red) and hDSG2 (green). Representative sections are shown. Scale bars, 20 μm.

mice, suggesting an hDSG2-independent uptake. Immunohistochemistry analyses showed that JO-1 in the liver is mostly present in sinusoidal spaces and F4/80-positive Kupffer cells (Supplementary Fig. S4) and not taken up by parenchymal liver cells. Similarly, in the spleen, JO-1 signals appear in the peripheral zone of germinal centers (Supplementary Fig. S4) and are mostly likely the result of uptake by splenic macrophages. The amount of JO-1 in the intestine and colon was more than 2-fold higher in hDSG2-transgenic mice without MMC-hDSG2 tumors, supporting our hypothesis that the tumor acts as a "sink" for JO-1. From the JO-1 biodistribution studies in MMC-hDSG2 tumor-bearing hDSG2 mice, the question arose why JO-1 predominantly accumulates in the tumor. Immunofluorescence studies on tumor and intestine sections of hDSG2-transgenic mice, showed that epithelial tumor cells lack strict polarization, in contrast to normal epithelial cells (Fig. 4E and F). As a consequence, in tumors, hDSG2 appears to be readily accessible, while in intestinal epithelial cells most of the hDSG2 is trapped in junctions, reflected by overlapping signals for hDSG2 and the junction marker claudin 7 (Fig. 4F).

We also measured clearance of JO-1 from blood after intravenous injection (Supplementary Fig. S5). These studies show that the half-life of JO-1 in hDSG2-transgenic mice

Published OnlineFirst April 24, 2012; DOI:10.1158/1078-0432.CCR-11-3213

is approximately 6 hours. JO-1 clearance from blood is slower in hDSG2-transgenic mice than in nontransgenic littermates, which could be due to the fact that hDSG2 is expressed on platelets and subfractions of leukocytes (12).

As JO-1 is a viral protein, adaptive immune responses might develop in humans, particularly after repeated injection. Despite the fact that approximately one third of humans have neutralizing antibodies against Ad3 (8), our studies showed that these antibodies did not interact with JO-1 (Fig. 5A). Furthermore, polyclonal anti–JO-1 antibodies generated by vaccination of mice did not affect the enhancing effect of JO-1 transepithelial transport of PEG 4000 in polarized colon cancer cultures (Fig. 5B). Our hDSG2-transgenic mouse/MMC-hDSG2 model allowed us to test the effect of anti–JO-1 antibodies on JO-1 activity *in vivo* (Fig. 5C). When JO-1 antibodies were detectable in serum of JO-1–vaccinated mice, MMC-hDSG2 tumor cells were injected into the mammary fat pad. As seen in the xenograft tumor models, JO-1 increased the efficacy of Doxil therapy in vaccinated, hDSG2-transgenic mice with preestablished MMC-hDSG2 tumors (Fig. 5C). Interestingly, JO-1 injection alone had a significant therapeutic effect in this immunocompetent tumor model. Because this effect was not seen in the immunodeficient tumor models (Fig. 1), we speculated that JO-1 facilitates antitumor immune responses. In support of this speculation, we found significantly more tumor-infiltrating leukocytes in MMC-hDSG2 tumor nests in JO-1–injected mice (Fig. 5E and F). Clearly, detailed T-cell studies are required to support this speculation. [Notably, MMC-hDSG2 cells express rat Neu (18), which could serve as an antigen.]

As seen before in hDSG2-transgenic mice that received intravenous Ad3-GFP injection, JO-1 injection also caused a mild diarrhea that started within 3 hours after injection and subsided by day 2. There were no significant changes in blood parameters at 24 hours (Supplementary Fig. 6A and B) and 3 days (not shown) after injection of JO-1 at a dose of 2 mg/kg, that is, a dose that conferred an enhancing effect on Doxil therapy. After injection of JO-1 at a dose of 10 mg/kg, blood analysis detected leucopenia, decrease in serum glucose levels, and increase in serum GPT levels. Liver damage is also reflected by the presence of steatosis in the liver (Supplementary Fig. S6C). Notably, the potential danger of provoking a serious immune response as a consequence of the administration of multiple doses of JO-1 to patients has to be taken into consideration.

Overall, our studies in hDSG2-transgenic mice show that JO-1 (2 mg/kg) cotherapy is safe and effective in the presence of anti–JO-1 antibodies.

Discussion

We showed that JO-1 cotherapy allows doses of chemotherapeutics to be decreased without compromising antitumor effects and that it provides protective effects to normal tissues resulting in an improved safety profile for chemotherapy. We also showed that JO-1 can overcome resistance of xenograft tumors to a chemotherapy drug. Our data indicate that JO-1 predominantly accumulates in tumors. A number of factors could account for this, including (i) overexpression of DSG2 on tumor cells, (ii) better accessibility of DSG2 on tumor cells because of a lack of strict cell polarization, and (iii) a high degree of vascularization and vascular permeability in tumors. Because of its preferential action on epithelial junctions of tumors, JO-1 appears to create as "sink" for chemotherapy drugs, thereby reducing the exposure of normal tissue to these drugs.

Before JO-1 cotherapy is used in cancer treatment, certain issues will need to be addressed.

JO-1 immunogenicity

This might not be a critical issue if JO-1 is used in combination with chemotherapy, which suppresses immune responses to foreign proteins (even at doses that are markedly lower than drug doses used for cancer treatment). This expectation is supported by studies with oncolytic adenovirus vectors in which immunosuppression allowed for repeated vector application (19). Furthermore, we have showed that JO-1 remains active *in vitro* and *in vivo* even in the presence of anti–JO-1 antibodies generated by vaccination of mice. This might be due to the fact that the JO-1 interaction with DSG2 is of very high avidity and cannot be disrupted by polyclonal anti–JO-1 antibodies. [Notably JO-1 is a dimer of a trimeric fiber knob (10)]. It can however not be excluded that repeated JO-1 injection into immunocompetent patients results in the development of competing, high-affinity antibodies. This problem can potentially be addressed by generating next generation JO-1 proteins that have immunodominant epitopes removed or higher affinity to DSG2. Furthermore, we have recently identified the DSG2-interacting residues within JO-1 and based on this knowledge, it might be possible to transplant the DSG2-interacting Ad3 fiber loops into less immunogenic scaffolds.

Role of DSG2 in cancers

In agreement with other studies (6, 7), we have found a higher DSG2 expression in malignant tissues than in the surrounding normal epithelial tissue (Supplementary Fig. S1). Furthermore, a recent study on squamous cell cancer showed that, in contrast to other desmosomal proteins, DSG2 was upregulated in invasive cancer (20). An National Center for Biotechnology Information website reports DSG2 expression in esophageal, colorectal, head and neck, kidney, uterine, bladder, prostate, gastrointestinal tract, breast, cervical, lung, ovarian, pancreatic, and skin tumors, whereas DSG2 was absent in adrenal tumors, sarcoma, glioma, leukemia, lymphoma, retinoblastoma, and soft tissue/muscle tissue tumors. (http://www.ncbi.nlm.nih.gov/UniGene/ESTProfileViewer.cgi?uglist = Hs.412597). There are, however, also studies reporting a reduction in the amounts of DSG2 in invasive pancreatic or gastric cancer (21, 22), and it has been argued that epithelial features,

Published OnlineFirst April 24, 2012; DOI:10.1158/1078-0432.CCR-11-3213

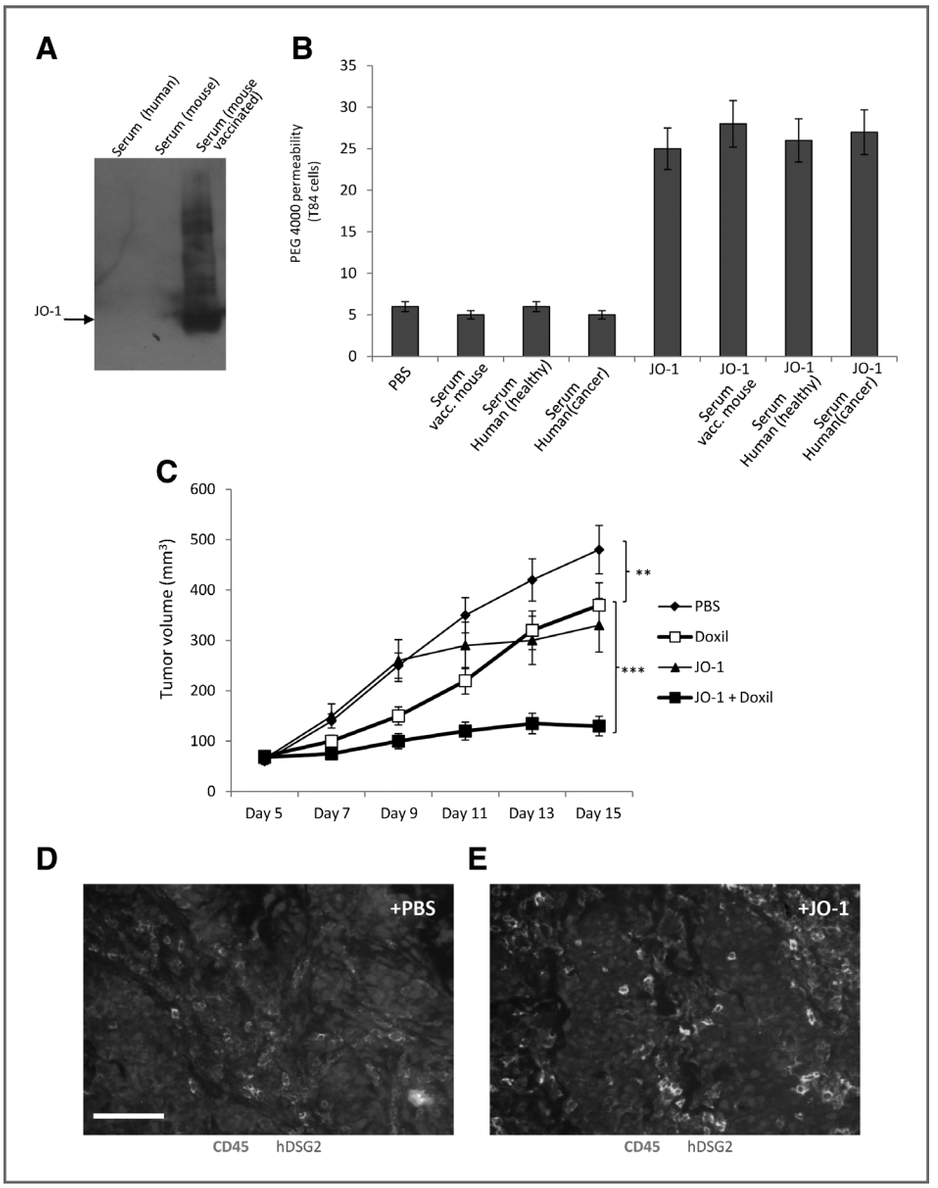

Figure 5. Effect of anti–JO-1 antibodies on JO-1 activity. A, analysis of serum for reactivity with JO-1 by Western blot. JO-1 was run on SDS-PAGE and filters were incubated with pooled human serum containing neutralizing antibodies against Ad3 virus (lane 1), serum from naïve mice (lane 2), or serum from JO-1–vaccinated mice (see Materials and Methods; lane 3). B, JO-1 enhances transepithelial transport of PEG (4,000 Da) *in vitro* in the presence of anti–JO-1 antibodies. Pooled serum from 10 healthy donors ("healthy") and 10 breast cancer patients ("cancer") or serum from a JO-1–vaccinated mouse ("vacc. mouse") was used in this study. Human colon epithelial T84 cells were incubated in Transwell plates until transepithelial resistance was constant. JO-1 (5 μg/mL) or PBS mixed with heat-inactivated serum (at a final concentration of 20%) was added to the inner chamber, followed by ^{14}C-PEG-4,000 1 hour later. Radioactive counts were measured 1 hour later in the outer chamber. $n = 3$. C, effect of JO-1 in vaccinated hDSG2-transgenic mice with MMC-hDSG2 tumors. Mice were vaccinated with JO-1 as described in (A). When JO-1 antibodies were detectable in serum, MMC-hDSG2 tumor cells were injected into the mammary fat pad. Treatment with JO-1 (2 mg/kg), Doxil (1.5 mg/kg), or JO-1 plus Doxil was started 5 days after tumor cell injection. $n = 5$. **, $P < 0.01$; ***, $P < 0.001$. D and E, MMC-hDSG2 tumor sections 2 days after PBS (D) or JO-1 (E) injection stained for the pan-leukocyte marker CD45 (bright). Scale bar, 20 μm. The number of CD45-positive cells in tumor nests was 7.8 (±3.4) cells/mm^2 in PBS-injected mice and 35 ± 12 cells/mm^2 in JO-1–injected mice ($n = 3$).

including tight junctions, are lost in metastatic cancer. These arguments do not consider that in advanced carcinomas mesenchymal cells can regain characteristics of epithelial cells via mesenchymal-to-epithelial transition (23). The epithelial phenotype of cancer cells and their ability to form physical barriers represent a protective mechanism for cancer cells. We have analyzed more than 60 primary and metastatic breast cancer samples and found overexpression of DSG2 in all of these samples. A fraction of these biopsies are shown in Supplementary Fig. S1.

Published OnlineFirst April 24, 2012; DOI:10.1158/1078-0432.CCR-11-3213

Risk of metastasis

JO-1 binding to DSG2 on tumor cells triggers pathways involved in epithelial-to-mesenchymal transition (EMT), a process which has been associated with tumor metastasis. However, to date none of our *in vivo* studies has shown any evidence of increased tumor growth or metastasis after treatment with JO-1. Furthermore, at day 3 after JO-1 injection into mice-bearing Her2/neu-positive HCC1954 tumors, there was no significant increase in the percentage of circulating Her2/neu-positive cells in the blood (Supplementary Fig. S7). Tumor metastasis requires more than transient activation of EMT pathways. Detachment from epithelial cancers and migration of tumor cells is only possible after long-term cross-talk between malignant cells and the tumor microenvironment, resulting in changes in the tumor stroma and phenotypic reprogramming of epithelial cells into mesenchymal cells (24).

Toxic side effects

Except for a mild, transient diarrhea, intravenous injection of JO-1 (at a dose of 2 mg/kg) had no critical side effects on other tissues or hematologic parameters in hDSG2-transgenic mice. We speculate that DSG2 in tissues other than the tumor and certain epithelial cells in the gastrointestinal tract is not accessible to intravenously injected JO-1. Clearly, the demonstration of safety of JO-1 in combination with chemotherapy drugs in non-human primates is required before this approach can be considered in humans. In this context, we have recently reported the DSG2 in macaques is expressed in the same patterns as in humans and that it is recognized by JO-1 (12).

Overall, we showed that JO-1 improves the efficacy and safety of a number of cancer chemotherapy drugs, implying that JO-1 cotherapy has the potential to improve the life quality of patients that receive cancer treatment. Moreover, it may allow patients to continue chemotherapy, which has been halted or delayed due to toxicity. Finally, cancer treatment with newer drugs, such as nab-paclitaxel and liposomal doxorubicin is expensive and presents a substantial burden to both patients and the costs of healthcare in general. JO-1 has potential to decrease costs of cancer therapy by reducing the amount of chemotherapy required as well as costs associated with treatment-related toxicity. These savings are likely to exceed the additional cost of JO-1 treatment.

Disclosure of Potential Conflicts of Interest

No potential conflicts of interest were disclosed.

Acknowledgments

The authors thank Melanie Wurm for helpful advice.

Grant Support

The study was supported by NIH grant R01 CA080192 (A. Lieber), R01 HLA078836 (A. Lieber), the Pacific Ovarian Cancer Research Consortium/Specialized Program of Research Excellence in Ovarian Cancer grant P50 CA83636, by a grant from the Fred Hutchinson Cancer Research Center, and a grant from the Marsha Rivkin Center for Ovarian Cancer Research. I. Beyer is a recipient of a postdoctoral fellowship award from "Deutsche Krebshilfe" (108988).

The costs of publication of this article were defrayed in part by the payment of page charges. This article must therefore be hereby marked *advertisement* in accordance with 18 U.S.C. Section 1734 solely to indicate this fact.

Received December 14, 2011; revised March 30, 2012; accepted April 12, 2012; published OnlineFirst April 24, 2012.

References

1. Lipinski CA, Lombardo F, Dominy BW, Feeney PJ. Experimental and computational approaches to estimate solubility and permeability in drug discovery and development settings. Adv Drug Deliv Rev 2001;46:3–26.
2. Lavin SR, McWhorter TJ, Karasov WH. Mechanistic bases for differences in passive absorption. J Exp Biol 2007;210:2754–64.
3. Green SK, Karlsson MC, Ravetch JV, Kerbel RS. Disruption of cell-cell adhesion enhances antibody-dependent cellular cytotoxicity: implications for antibody-based therapeutics of cancer. Cancer Res 2002;62:6891–900.
4. Fessler SP, Wotkowicz MT, Mahanta SK, Bamdad C. MUC1* is a determinant of trastuzumab (Herceptin) resistance in breast cancer cells. Breast Cancer Res Treat 2009;118:113–24.
5. Oliveras-Ferraros C, Vazquez-Martin A, Cufi S, Queralt B, Baez L, Guardeno R, et al. Stem cell property epithelial-to-mesenchymal transition is a core transcriptional network for predicting cetuximab (Erbitux) efficacy in KRAS wild-type tumor cells. J Cell Biochem 2011;112:10–29.
6. Biedermann K, Vogelsang H, Becker I, Plaschke S, Siewert JR, Hofler H, et al. Desmoglein 2 is expressed abnormally rather than mutated in familial and sporadic gastric cancer. J Pathol 2005;207:199–206.
7. Harada H, Iwatsuki K, Ohtsuka M, Han GW, Kaneko F. Abnormal desmoglein expression by squamous cell carcinoma cells. Acta Derm Venereol 1996;76:417–20.
8. Wang H, Li ZY, Liu Y, Persson J, Beyer I, Moller T, et al. Desmoglein 2 is a receptor for adenovirus serotypes 3, 7, 11 and 14. Nat Med 2011;17:96–104.
9. Trinh HV, Lesage G, Chennamparampil V, Vollenweider B, Burckhardt CJ, Schauer S, et al. Avidity binding of human adenovirus serotypes 3 and 7 to the membrane cofactor CD46 triggers infection. J Virol 2012;86:1623–37.
10. Wang H, Li Z, Yumul R, Lara S, Hemminki A, Fender P, et al. Multimerization of adenovirus serotype 3 fiber knob domains is required for efficient binding of virus to desmoglein 2 and subsequent opening of epithelial junctions. J Virol 2011;85:6390–402.
11. Beyer I, van Rensburg R, Strauss R, Li Z, Wang H, Persson J, et al. Epithelial junction opener JO-1 improves monoclonal antibody therapy of cancer. Cancer Res 2011;71:7080–90.
12. Wang H, Beyer I, Persson J, Song H, Li Z, van Rensburg R, et al. A new human DSG2-transgenic mouse model for studying the tropism and pathology of DSG2-interacting adenoviruses. J Virol 2012;86:6286–302.
13. Su YC, Chen BM, Chuang KH, Cheng TL, Roffler SR. Sensitive quantification of PEGylated compounds by second-generation anti-poly(ethylene glycol) monoclonal antibodies. Bioconjug Chem 2010;21:1264–70.
14. Beyer I, van Rensburg R, Strauss R, Li Z, Wang H, Persson J, et al. Epithelial junction opener JO-1 improves monoclonal antibody therapy of cancer. Cancer Res 2011;71:7080–90.

Published OnlineFirst April 24, 2012; DOI:10.1158/1078-0432.CCR-11-3213

15. Sugahara KN, Teesalu T, Karmali PP, Kotamraju VR, Agemy L, Greenwald DR, et al. Coadministration of a tumor-penetrating peptide enhances the efficacy of cancer drugs. Science 2010;328:1031–5.
16. Strauss R, Li ZY, Liu Y, Beyer I, Persson J, Sova P, et al. Analysis of epithelial and mesenchymal markers in ovarian cancer reveals phenotypic heterogeneity and plasticity. PLoS One 2011;6:e16186.
17. Emmenegger U, Francia G, Chow A, Shaked Y, Kouri A, Man S, et al. Tumors that acquire resistance to low-dose metronomic cyclophosphamide retain sensitivity to maximum tolerated dose cyclophosphamide. Neoplasia 2011;13:40–8.
18. Knutson KL, Almand B, Dang Y, Disis ML. Neu antigen-negative variants can be generated aftaer neu-specific antibody therapy in neu transgenic mice. Cancer Res 2004;64:1146–51.
19. Thomas MA, Spencer JF, Toth K, Sagartz JE, Phillips NJ, Wold WS. Immunosuppression enhances oncolytic adenovirus replication and antitumor efficacy in the Syrian hamster model. Mol Ther 2008;16:1665–73.
20. Kurzen H, Munzing I, Hartschuh W. Expression of desmosomal proteins in squamous cell carcinomas of the skin. J Cutan Pathol 2003;30:621–30.
21. Ramani VC, Hennings L, Haun RS. Desmoglein 2 is a substrate of kallikrein 7 in pancreatic cancer. BMC Cancer 2008;8:373.
22. Yashiro M, Nishioka N, Hirakawa K. Decreased expression of the adhesion molecule desmoglein-2 is associated with diffuse-type gastric carcinoma. Eur J Cancer 2006;42:2397–403.
23. Christiansen JJ, Rajasekaran AK. Reassessing epithelial to mesenchymal transition as a prerequisite for carcinoma invasion and metastasis. Cancer Res 2006;66:8319–26.
24. Guarino M. Epithelial-mesenchymal transition and tumour invasion. Int J Biochem Cell Biol 2007;39:2153–60.